Improved 2-step QRM-ML Block Signal Detection for Single-Carrier Transmission

Katsuhiro TEMMA† Tetsuya YAMAMOTO† and Fumiyuki ADACHI‡
Dept. of Electrical and Communication Engineering, Graduate School of Engineering, Tohoku University
6-6-05 Aza-Aoba, Aramaki, Aoba-ku, Sendai, 980-8579 Japan
†{tenma, yamamoto}@mobile.ecei.tohoku.ac.jp, ‡adachi@ecei.tohoku.ac.jp

***Abstract*—A new 2-step maximum likelihood block signal detection employing QR decomposition and M-algorithm (QRM-MLBD) is proposed to further reduce the computational complexity while keeping a good bit error rate (BER) performance for the single-carrier (SC) transmission in a frequency-selective fading channel. Prior to QRM-MLBD, a computationally efficient minimum mean square error based frequency-domain equalization (MMSE-FDE) is performed to discard the symbol candidates in the tree based on the soft decision results of MMSE-FDE. We evaluate, by computer simulation, the BER performance achievable by the proposed improved 2-step QRM-MLBD and show that the proposed scheme can reduce the computational complexity compared to the previously proposed conventional 2-step QRM-MLBD while keeping the same BER performance.**

Keywords-component; Single-carrier, block signal detection, MMSE-FDE, QR decomposition, M-algorithm

I. INTRODUCTION

The broadband wireless channel is composed of many propagation paths with different time delays and therefore, the channel becomes severely frequency-selective [1]. A low computational complexity minimum mean square error based frequency-domain equalization (MMSE-FDE) can significantly improve the bit error rate (BER) performance of single-carrier (SC) transmission [2, 3]. However, a big performance gap from the matched filter (MF) bound still exists due to the presence of the residual inter-symbol interference (ISI) after FDE [4]. Although the maximum likelihood detection (MLD) [5] is the optimum signal detection, its computational complexity is enormously high.

A maximum likelihood block signal detection employing QR decomposition and M-algorithm (QRM-MLBD) [6] for the reception of the SC signals transmitted over a frequency-selective fading channel was proposed [7, 8]. QRM-MLBD can achieve the BER performance close to the MF bound with less complexity compared to MLD. However, its computational complexity is still high. Recently, in order to further reduce the complexity, we proposed a 2-step QRM-MLBD [9] which discards unreliable symbol candidates in the tree by using MMSE-FDE tentative decision. However, the complexity reduction is limited.

In this paper, we propose the improved 2-step QRM-MLBD. Instead of using hard decision of MMSE-FDE, soft decision is used to discard unreliable symbol candidates in the tree. The MMSE-FDE output is modeled as a Gaussian variable and the symbol candidates are selected based on the Euclidean distance from the MMSE-FDE output.

The remainder of this paper is organized as follows. Sect. II presents the improved 2-step QRM-MLBD for SC transmission. In Sect. III, the average BER performance and computational complexity of the improved 2-step QRM-MLBD in a frequency-selective fading channel are evaluated by computer simulation. Sect. IV offers the conclusion.

II. SC TRANSMISSION USING IMPROVED 2-STEP QRM-MLBD

The SC transmission model is illustrated in Fig. 1. Throughout the paper, the T_s symbol-spaced discrete time representation is used. We assume a symbol-spaced frequency-selective fading channel composed of L distinct propagation paths. The received signal is a cyclic convolution of the transmitted signal block and the channel impulse response as long as the cyclic prefix (CP) is longer than the maximum channel time delay.

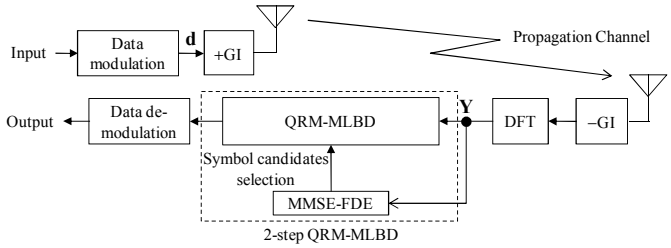

Figure 1. SC transmission model.

A. Received Signal

A block of N_c symbols is assumed to be transmitted. In this paper, the data symbol block is expressed using the vector form as $\mathbf{d}=[d(0),\ldots,d(N_c-1)]^T$ ($[.]^T$ denotes the transpose operation). The last N_g symbols of each block are copied as a CP and inserted into the guard interval (GI) placed at the beginning of each block.

At the receiver, N_c-point discrete Fourier transform (DFT) is applied to transform the received signal into the frequency-domain signal. The frequency-domain received signal $\mathbf{Y}=[Y(0),\ldots,Y(N_c-1)]^T$ can be represented as

$$\mathbf{Y}=\sqrt{\frac{2E_s}{T_s}}\mathbf{H}\mathbf{d}+\mathbf{N}, \tag{1}$$

where E_s is the symbol energy. $\mathbf{H}=diag[H(0),\ldots,H(N_c-1)]$ represents the frequency-domain channel gain matrix and $H(k)=\sum_{l=0}^{L-1}h_l\exp(-j2\pi k\tau_l/N_c)$, where h_l and τ_l are the complex-valued path gain with $E[\sum_{l=0}^{L-1}|h_l|^2]=1$ and the time delay of the lth path, respectively. $\mathbf{N}=[N(0),\ldots,N(N_c-1)]^T$ is the

frequency-domain noise vector whose elements are independent zero-mean additive white Gaussian variables having the variance $2N_0/T_s$, N_0 is the one-sided power spectrum density of the additive white Gaussian noise (AWGN). **F** is the DFT matrix given by

$$\mathbf{F}=\frac{1}{\sqrt{N_c}}\begin{bmatrix}1 & 1 & \cdots & 1\\ 1 & e^{-j2\pi\frac{1\times 1}{N_c}} & \cdots & e^{-j2\pi\frac{1\times(N_c-1)}{N_c}}\\ \vdots & \vdots & \ddots & \vdots\\ 1 & e^{-j2\pi\frac{(N_c-1)\times 1}{N_c}} & \cdots & e^{-j2\pi\frac{(N_c-1)\times(N_c-1)}{N_c}}\end{bmatrix}. \quad (2)$$

B. QRM-MLBD

A concatenation of propagation channel **H** and DFT matrix **F** can be viewed as an equivalent channel $\overline{\mathbf{H}}=\mathbf{HF}$. By applying the QR decomposition to the equivalent channel matrix as $\overline{\mathbf{H}}=\mathbf{QR}$, where **Q** is an $N_c\times N_c$ unitary matrix and **R** is an $N_c\times N_c$ upper triangular matrix and then multiplying **Y** by $\mathbf{Q}^H$, the transformed frequency-domain received signal **Z** is obtained as

$$\begin{aligned}\mathbf{Z}=[Z(0),\cdots,Z(N_c-1)]^T&=\mathbf{Q}^H\mathbf{Y}=\sqrt{\frac{2E_s}{T_s}}\mathbf{Rd}+\mathbf{Q}^H\mathbf{N}\\&=\sqrt{\frac{2E_s}{T_s}}\begin{bmatrix}R_{0,0} & \cdots & R_{0,N_c-1}\\ & \ddots & \vdots\\ \mathbf{0} & & R_{N_c-1,N_c-1}\end{bmatrix}\begin{bmatrix}d(0)\\ \vdots\\ d(N_c-1)\end{bmatrix}+\mathbf{Q}^H\mathbf{N}\end{aligned}. \quad (3)$$

From Eq. (3), the ML decision on the transmitted block can be efficiently performed by searching for the best path having the minimum Euclidean distance in the tree diagram composed of N_c stages as shown in Fig. 2. However, we need a full tree-search for obtaining ML solution and it leads to very high computational complexity. Therefore, in QRM-MLBD, the M-algorithm [10] is used in order to reduce the complexity of tree-search. However, its computational complexity is still high.

The complexity of QRM-MLBD is spent to compute the path metric in tree-search. Hence, by discarding unreliable symbol candidates in the tree before searching, the computational complexity can be reduced. Recently, we proposed a 2-step QRM-MLBD [9]. MMSE-FDE tentative decision is carried out prior to QRM-MLBD to discard unreliable symbol candidates in the tree. However, the complexity reduction is limited. Below, we propose an improved 2-step QRM-MLBD. Instead of using the hard decision results of MMSE-FDE, the soft decision results are used to discard unreliable symbol candidates in the tree.

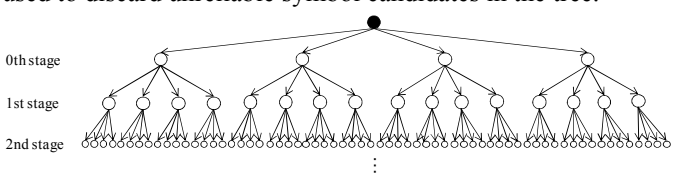

Figure 2. Tree structure of QRM-MLBD (QPSK case).

C. Improved 2-step QRM-MLBD

In the first step, MMSE-FDE is carried out by multiplying **Y** by the MMSE weight matrix **W** as [2, 3]

$$\widetilde{\mathbf{D}}=\mathbf{WY}\ , \quad (4)$$

where

$$\begin{cases}\mathbf{Y}=\sqrt{\frac{2E_s}{T_s}}\mathbf{HD}+\mathbf{N}\\ \mathbf{W}=diag\left[\frac{H^*(0)}{|H(0)|^2+N_0/E_s},\cdots,\frac{H^*(N_c-1)}{|H(N_c-1)|^2+N_0/E_s}\right]\end{cases}, \quad (5)$$

D=Fd is the frequency-domain transmitted signal vector and $[.]^*$ denotes the complex conjugate operation. Next, applying N_c-point inverse DFT (IDFT) to $\widetilde{\mathbf{D}}=[\widetilde{D}(0),\ldots,\widetilde{D}(N_c-1)]^T$, the soft decision symbol vector $\widetilde{\mathbf{d}}=[\widetilde{d}(0),\ldots,\widetilde{d}(N_c-1)]^T$ is obtained as

$$\widetilde{\mathbf{d}}=\mathbf{F}^H\widetilde{\mathbf{D}}, \quad (6)$$

which is used for discarding unreliable symbol candidates.

The soft decision symbol $\widetilde{d}(t)$ can be expressed as

$$\widetilde{d}(t)=\sqrt{\frac{2E_s}{T_s}}\left(\frac{1}{N_c}\sum_{k=0}^{N_c-1}\widetilde{H}(k)\right)d(t)+\mu_{ISI}(t)+\mu_{noise}(t), \quad (7)$$

where $\widetilde{H}(k)=W(k)H(k)$ is the frequency-domain channel gain at the kth frequency after MMSE-FDE. In Eq. (7), the first, second, and third terms are the desired signal, residual ISI, and noise components, respectively. $\widetilde{d}(t)$ is normalized by $A=\sqrt{2E_s/T_s}\{(1/N_c)\sum_{k=0}^{N_c-1}\widetilde{H}(k)\}$ as

$$\widetilde{d}'(t)=d(t)+\mu'_{ISI}(t)+\mu'_{noise}(t), \quad (8)$$

where the second and third terms are given as

$$\begin{cases}\mu'_{ISI}(t)=A^{-1}\sqrt{\frac{2E_s}{T_s}}\frac{1}{N_c}\sum_{k=0}^{N_c-1}\widetilde{H}(k)\left[\sum_{n=0\neq t}^{N_c-1}d(n)\exp\left(j2\pi k\frac{t-n}{N_c}\right)\right]\\ \mu'_{noise}(t)=A^{-1}\frac{1}{N_c}\sum_{k=0}^{N_c-1}\widetilde{N}(k)\exp\left(j2\pi k\frac{t}{N_c}\right)\end{cases} \quad (9)$$

with $\widetilde{N}(k)=W(k)N(k)$ denoting the noise component at the kth frequency after MMSE-FDE.

It can be understood from Eq. (8) that $\widetilde{d}'(t)$ is a complex random variable having the mean $d(t)$. The symbol candidates are selected based on the Euclidean distance from $\widetilde{d}'(t)$. In this paper, $\mu'_{ISI}(t)$ and $\mu'_{noise}(t)$ are modeled as independent zero-mean complex Gaussian variables. The residual ISI plus noise component $\mu(t)=\mu'_{ISI}(t)+\mu'_{noise}(t)$ can be treated as a new zero-mean complex Gaussian variable [11]. The variance σ_μ^2 of $\mu(t)$ is given by

$$\sigma_\mu^2=\frac{1}{2}E[|\mu(t)|^2]=\sigma_{ISI}^2+\sigma_{noise}^2. \quad (10)$$

From Eq. (9), σ_{ISI}^2 and σ_{noise}^2 can be derived as [11]

$$\begin{cases} \sigma_{ISI}^2 = A^{-2}\dfrac{E_s}{T_s}\left[\dfrac{1}{N_c}\sum_{k=0}^{N_c-1}\left|\widetilde{H}(k)\right|^2 - \left|\dfrac{1}{N_c}\sum_{k=0}^{N_c-1}\widetilde{H}(k)\right|^2\right] \\ \sigma_{noise}^2 = A^{-2}\dfrac{1}{N_c}\dfrac{N_0}{T_s}\sum_{k=0}^{N_c-1}\left|W(k)\right|^2 \end{cases}. \quad (11)$$

The probability density function (pdf) of the distance r between the MMSE-FDE output $\widetilde{d}'(t)$ and its mean $d(t)$ is given as

$$p(r) = \frac{r}{\sigma_\mu^2}\exp\left(-\frac{r^2}{2\sigma_\mu^2}\right). \quad (12)$$

In the proposed improved 2-step QRM-MLBD, the symbol candidate selection is performed by drawing the circle centered at each symbol candidates in the signal constellation. The radius of the circle is determined using the pdf of r. The radius R_β of the circle, outside which r falls with the probability β, is given as

$$R_\beta = \sqrt{-2\sigma_\mu^2 \ln\beta}\,. \quad (13)$$

The circle is drawn centered each symbol candidate and the symbol candidates whose distance from the normalized soft decision output of MMSE-FDE is shorter than R_β are selected as reliable ones and others are discarded as unreliable ones, as shown in Fig. 3(a). Also, there is a possibility that none of the symbols is selected as Fig. 3(b). In this paper, only the hard decision result of MMSE-FDE is selected in such cases.

D. Optimization of β

If β is set too large (i.e., close to unity), none of symbols may be found as shown in Fig. 3(b). The value of β depends on the channel condition, modulation level, and average received signal energy per bit-to-AWGN power spectrum density ratio E_b/N_0. It is quite difficult, if not impossible, to theoretically find the optimum β that can achieve the near MF bound performance. In this paper, we found, by the preliminary computer simulation, the optimum β at each average received E_b/N_0 for the given channel power delay profile and data modulation.

E. Complexity Consideration

After the symbol selection, there may be some symbols which have no candidate symbol selected or only one candidate symbol (i.e., $N_{cand}^{(i)}=1$, where $N_{cand}^{(i)}$ denotes the number of symbol candidates selected for the ith symbol $d(i)$). If $N_{cand}^{(i)}=1$, the ith stage can be removed from the frequency-domain received signal $\mathbf{Y}$ before applying the QR decomposition to the equivalent channel matrix as

$$\hat{\mathbf{Y}} = \sqrt{\frac{2E_s}{T_s}}\hat{\mathbf{H}}\hat{\mathbf{d}} + \mathbf{N} = \mathbf{Y} - \sqrt{\frac{2E_s}{T_s}}\overline{\mathbf{H}}\,\overline{\mathbf{d}}\,, \quad (14)$$

where $\overline{\mathbf{d}} = [0,\ldots,0,\overline{d}(i),0,\ldots,0]^T$ with $\overline{d}(i)$ being the ith symbol of hard decision MMSE-FDE and other elements being 0. From Eq. (14), their corresponding columns of $\overline{\mathbf{H}}$ can be removed as shown in Fig.4 (a). Therefore, the size of equivalent channel matrix can be reduced from $N_c\times N_c$ to $N_c\times(N_c-C)$, where C is the number of stages with $N_{cand}^{(i)}=1$. Noting that the number of complex multiply operations required for the Gram-Schmidt QR decomposition of a matrix of size $A\times B$ is $A\times B^2$, the number of complex multiply operations in QR decomposition can be reduced from N_c^3 to $N_c(N_c-C)^2$. In addition, the number of stages of M-algorithm can be reduced from N_c to N_c-C in improved 2-step QRM-MLBD as in Fig.4 (b) because the stages with $N_{cand}^{(i)}=1$ are removed in Eq. (14). Therefore, the improved 2-step QRM-MLBD reduces the computational complexity compared to conventional 2-step QRM-MLBD.

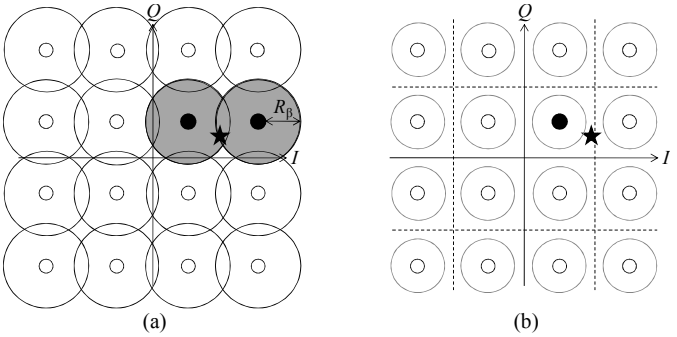

Figure 3. Symbol candidate selection in improved 2-step QRM-MLBD.

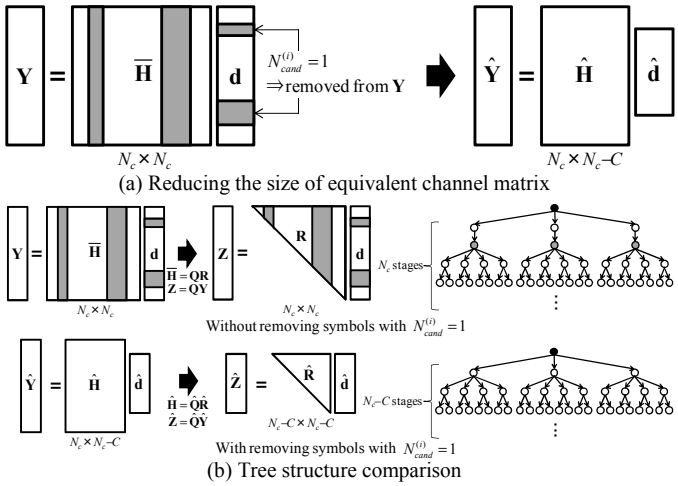

Figure 4. Reducing the size of equivalent channel matrix and the tree structure of improved 2-step QRM-MLBD.

III. Computer Simulation

First, we evaluate the number $N_{cand}^{(i)}$ of selected symbol candidates associated with the ith symbol $d(i)$ of the proposed improved 2-step QRM-MLBD. Then, we evaluate the average BER performance and computational complexity by computer simulation. The computer simulation condition is as below. We assume 16QAM data modulation, block size N_c=64, and GI size N_g=16. The channel is assumed to be a frequency-selective block Rayleigh fading channel having symbol-spaced L=16-path uniform power delay profile. Ideal channel estimation is assumed.

A. The Number of $N_{cand}^{(i)}$

Figure 5 plots the average $N_{cand}^{(i)}$ per stage (= $(1/N_c)\sum_{i=0}^{N_c-1}N_{cand}^{(i)}$) as a function of the average received E_b/N_0

(=(E_s/N_0)(1+N_g/N_c)/$\log_2 X$, where X is the modulation level) for the conventional and improved 2-step QRM-MLBDs. Note that for the QRM-MLBD, $N_{cand}^{(i)}$ is always equal to the modulation level X. For the conventional 2-step QRM-MLBD, the average $N_{cand}^{(i)}$ is 6.25 (which is the average when X symbols are transmitted with equal probability) for 16QAM [9]. From Fig. 5, it can be seen that the proposed improved 2-step QRM-MLBD can reduce the average $N_{cand}^{(i)}$ compared to the conventional 2-step QRM-MLBD. It can be also seen that the maximum value of average number of symbol candidates per stage (defined as the average of $N_{cand}^{(i)}$ over i=0~63) is larger for the improved 2-step QRM-MLBD than for the conventional 2-step QRM-MLBD. However, the probability that the average $N_{cand}^{(i)}$ per stage for the improved 2-step QRM-MLBD becomes larger than that for the conventional 2-step QRM-MLBD (i.e., 6.25) is quite low as shown in Fig. 6.

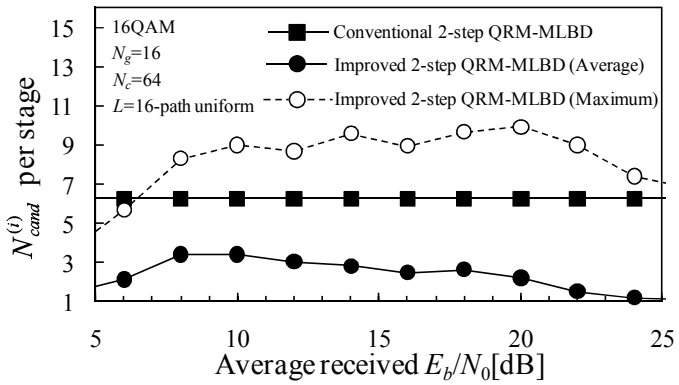

Figure 5. Average $N_{cand}^{(i)}$ per stage.

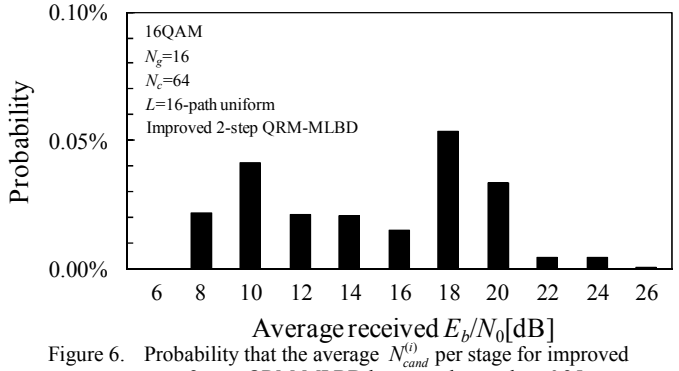

Figure 6. Probability that the average $N_{cand}^{(i)}$ per stage for improved 2-step QRM-MLBD becomes larger than 6.25

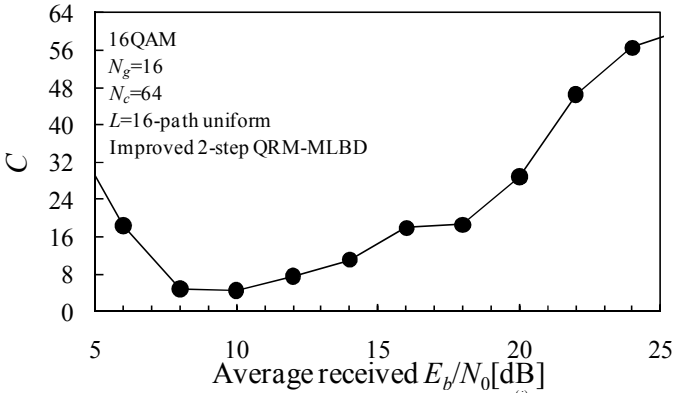

Figure 7. Average number C of stages with $N_{cand}^{(i)}=1$ after symbol selection in the first step.

Figure 7 plots the average number C of stages with $N_{cand}^{(i)}=1$ after symbol selection in the first step. It can be seen from Fig. 7 that many stages with $N_{cand}^{(i)}=1$ exist and therefore, the computational complexity of QR decomposition can be reduced.

It can be seen from Fig. 5 that the average $N_{cand}^{(i)}$ is higher in a moderate E_b/N_0 region than in low and high E_b/N_0 regions. In a low E_b/N_0 region, the BER difference between QRM-MLBD and MMSE-FDE is very small. Thus, a small number of symbol candidates are selected. When E_b/N_0 goes high, the BER difference becomes wider and therefore, the average $N_{cand}^{(i)}$ increases. In a high E_b/N_0 region, however, since the BER of MMSE-FDE reduces sufficiently, only a small number of symbol candidates remain.

B. Average BER Performance and Computational Complexity

Figure 8(a) compares the improved and conventional 2-step QRM-MLBDs. Fig. 8(b) compares the improved 2-step and original QRM-MLBDs. Both the improved and conventional 2-step QRM-MLBDs can achieve almost the same BER performance as the original QRM-MLBD when the same value of M is used. Therefore, an interesting question is to which extent the computational complexity can be reduced by the improved 2-step QRM-MLBD.

The computational complexity of the improved 2-step QRM-MLBD per block of N_c symbols is evaluated in terms of the number of complex multiply operations required to achieve the near MF bound performance. The number of complex multiplications is compared to the original QRM-MLBD in Fig. 9. In Table I, the number of multiply operations is shown. The improved 2-step QRM-MLBD involves MMSE-FDE, computation of radius R_β, symbol candidate selection and subtraction of $\bar{d}(i)$ from $\mathbf{Y}$ at the stages with $N_{cand}^{(i)}=1$ in addition to QRM-MLBD. However, the improved 2-step QRM-MLBD significantly reduces the computational complexity required for QR decomposition and path metric calculation. Therefore, a total computational complexity of improved 2-step QRM-MLBD is greatly reduced compared to QRM-MLBD and the conventional 2-step QRM-MLBD. The improved 2-step QRM-MLBD requires only 10% (23%) of the average complexity for achieving average BER=10^{-5} compared to QRM-MLBD (conventional 2-step QRM-MLBD) in the case of 16QAM.

IV. CONCLUSIONS

In this paper, we proposed the improved 2-step QRM-MLBD which utilizes the soft decision results of MMSE-FDE for the selection of the reliable candidate symbols in the first step in order to reduce the complexity of QRM-MLBD in the second step. We showed that the improved 2-step QRM-MLBD can reduce the average computational complexity to about 10% of the original QRM-MLBD and 23% of the conventional 2-step QRM-MLBD for 16QAM.

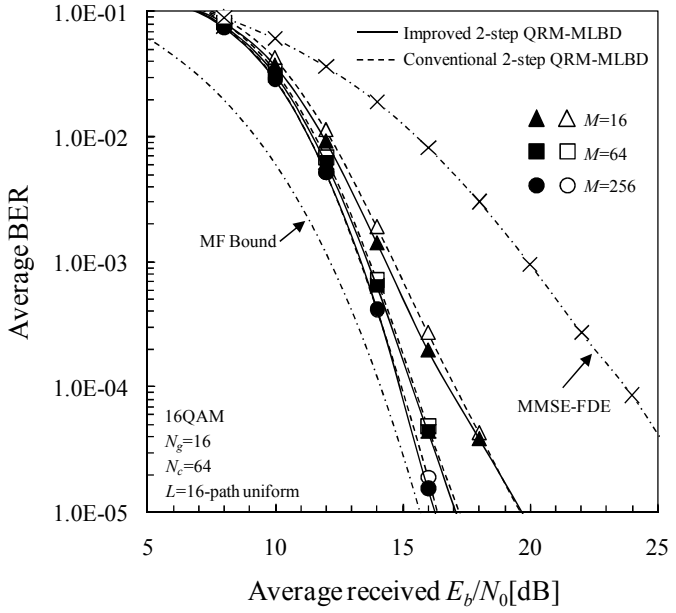

(a) Improved and conventional 2-step QRM-MLBDs

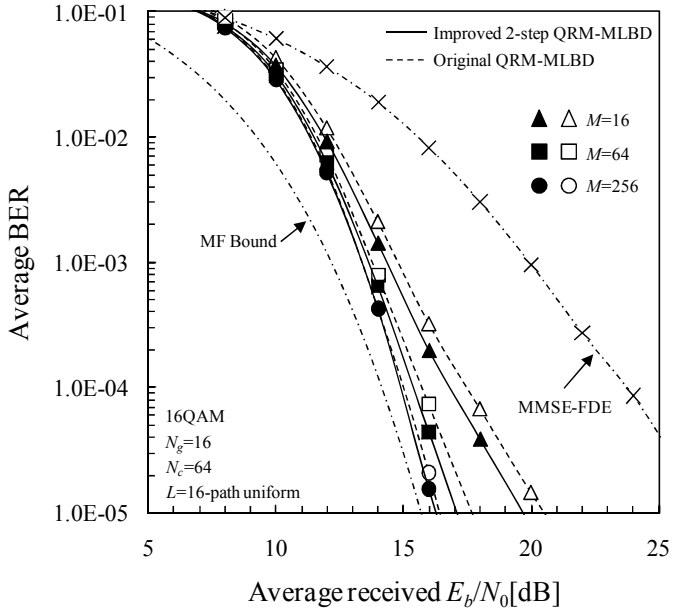

(b) Improved 2-step QRM-MLBD and original QRM-MLBD

Figure 8. Average BER performance comparison.

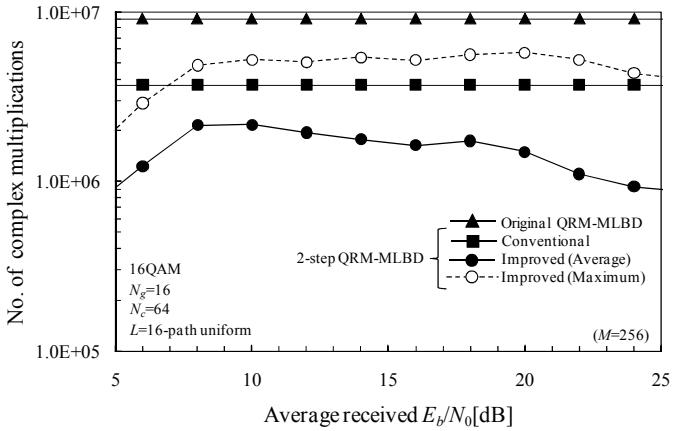

Figure 9. Complexity comparison

TABLE I. NUMBER OF COMPLEX MULTIPLY OPERATIONS

	QRM-MLBD	2-step QRM-MLBD	
		Conventional	Improved
Fast Fourier transform (FFT)	$N_c\log_2 N_c$	$N_c\log_2 N_c$	$N_c\log_2 N_c$
MMSE-weight computation & FDE		$2N_c$	$2N_c$
Inverse FFT (IFFT)		$N_c\log_2 N_c$	$N_c\log_2 N_c$
Computation of **HF**	N_c^2	N_c^2	N_c^2
Computation of R_β			$3N_c+1$
Symbol candidate selection			$2XN_c$
Subtraction of $\bar{d}(i)$ from **Y**			CN_c
QR decomposition	N_c^3	N_c^3	$N_c(N_c-C)^2$
Computation of $\mathbf{Q}^H\mathbf{Y}$	N_c^2	N_c^2	$N_c(N_c-C)$
Path metric computation	$X\{2+(M/2)(N_c+4)(N_c-1)\}$	$E[N_{cand}^{(i)}]\{2+(M/2)(N_c+4)(N_c-1)\}$	$E[N_{cand}^{(i)}]\{2+(M/2)(N_c-C+4)(N_c-C-1)\}$

REFERENCES

[1] J. G. Proakis and M. Salehi, *Digital communications*, 5th ed., McGraw-Hill, 2008.

[2] D. Falconer, S. L. Ariyavisitakul, A. Benyamin- Seeyar, and B. Edison, "Frequency domain equalization for single-carrier broadband wireless systems," IEEE Commun. Mag., Vol. 40, No. 4, pp. 58-66, Apr. 2002..

[3] F. Adachi, T. Sao, and T. Itagaki, "Performance of multicode DS-CDMA using frequency domain equalization in a frequency selective fading channel," IEE Electronics Letters, Vol. 39, No.2, pp. 239-241, Jan. 2003.

[4] K. Takeda, K. Ishihara, and F. Adachi, "Frequency-domain ICI cancellation with MMSE equalization for DS-CDMA downlink," IEICE Trans. Commun., Vol. E89-B, No. 12, pp. 3335-3343, Dec. 2006.

[5] A. van Zelst, R. van Nee, and G. A. Awater, "Space division multiplexing (SDM) for OFDM systems," Proc. IEEE 51st Vehicular Technology Conference (VTC), pp. 1070-1074, May 2000.

[6] L. J. Kim and J. Yue, "Joint channel estimation and data detection algorithms for MIMO-OFDM systems," Proc. Thirty-Sixth Asilomar Conference on Signals, System and Computers, pp. 1857-1861, Nov. 2002.

[7] K. Nagatomi, K. Higuchi, and H. Kawai "Complexity reduced MLD based on QR decomposition in OFDM MIMO multiplexing with frequency domain spreading and code multiplexing," Proc. IEEE Wireless Communications and Networking Conference (WCNC 2009), pp. 1-6, Apr. 2009.

[8] T. Yamamoto, K. Takeda, and F. Adachi, "Single-carrier transmission using QRM-MLD with antenna diversity," Proc. The 12th International Symposium on Wireless Personal Multimedia Communications (WPMC 2009), Sendai, Japan, Sept. 2009.

[9] K. Temma, T. Yamamoto, and F. Adachi, "Computationally efficient 2-step QRM-MLD for single-carrier transmissions," Proc. The IEEE International Conference on Communication Systems (IEEE ICCS 2010), Singapore, 17-19, Nov. 2010.

[10] J. B. Anderson and S. Mohan, "Sequential coding algorithms: A survey and cost analysis," IEEE Trans. on Commun., Vol. 32, pp. 169-176, Feb. 1984.

[11] F. Adachi and K. Takeda, "Bit error rate analysis of DS-CDMA with joint frequency-domain equalization and antenna diversity combining," IEICE Trans. Commun., Vol. E87-B, No. 10, pp.2991-3002, Oct. 2004.